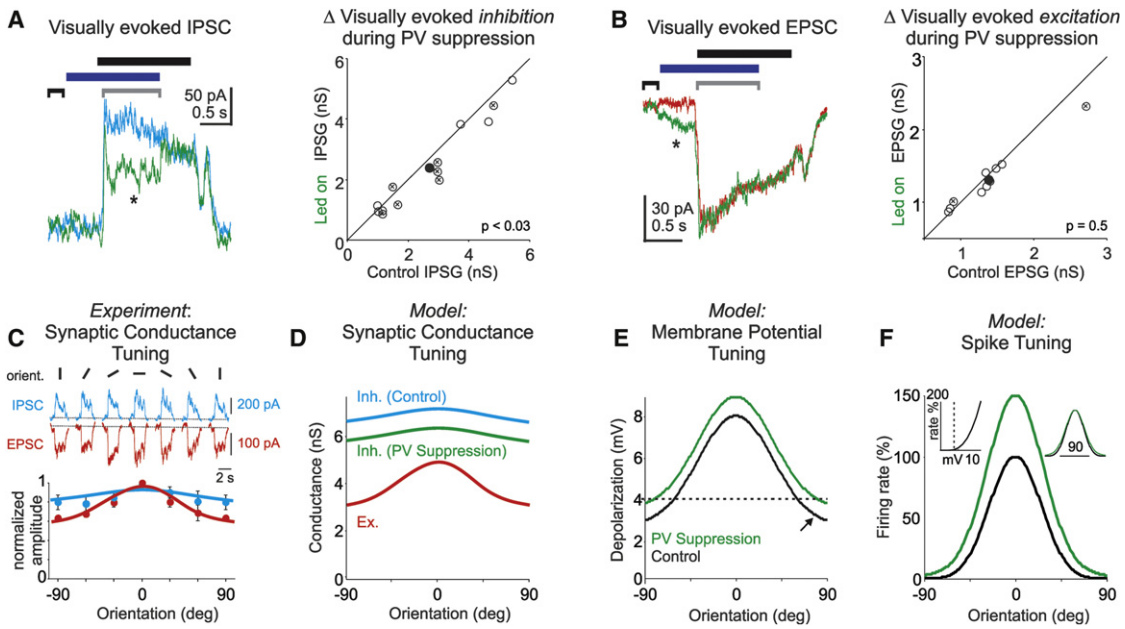

Figure 5. A Model Based on Experimentally Determined Synaptic Conductances Captures Linear Transformation of Pyr Cell Responses

(A) Left: visually evoked inhibitory postsynaptic currents (IPSC) recorded in a Pyr cell during control (cyan) and PV cell suppression (green). Average of 38 sweeps at each condition. Horizontal bars: black, stimulus presentation; blue, LED illumination. Brackets: black, baseline; gray, time over which average IPSC amplitude is computed. Right: scatter plot of visually evoked inhibitory conductance in control versus during PV cell photo suppression (open circles); "X" marks individual cells with significant change in conductance. Solid circle illustrates mean. Average decrease ~10%; n = 13; $p < 0.03$.

(B) Left: visually evoked excitatory postsynaptic currents (EPSC) recorded in a Pyr cell during control (red) and PV cell photo suppression (green). Average of 62 sweeps at each condition; horizontal bars and brackets as above. Note that while there is no change in the visually evoked EPSCs relative to baseline (black bracket), a significant increase in EPSC amplitude occurred systematically at led onset (asterisk; 0.1 ± 0.02 nS; n = 10; $p < 0.004$). Right: scatter plot of visually evoked excitatory conductance in control versus during PV cell photo suppression (open circles); "X" marks individual cells with significant change in conductance; solid circle illustrates mean. Excitatory conductance did not change significantly; n = 10; $p = 0.5$).

(C) Top: visually evoked IPSCs (cyan) and EPSCs (red) recorded in a layer 2/3 Pyr cell during the presentation of six sinusoidal grating orientations.

Bottom, dots: summary of excitatory (red; n = 4) and inhibitory (cyan; n = 5) tuning as a function of orientation. Error bars are the SEM. Lines are the respective Gaussian fits.

(D) Tuning of excitatory synaptic conductance (red) and inhibitory synaptic conductance (cyan: control; green: during PV cell suppression, i.e., 10% reduction) as a function of orientation. Lines are the Gaussian fits from (C).

(E) Net depolarization in the membrane potential of modeled cell (resulting from conductances in D) as a function of orientation under control conditions (black) and during PV cell suppression (green). The dotted line illustrates the spike threshold. Note that under control conditions the membrane potential is above threshold at most orientations.

(F) Model cell's orientation tuning, i.e., firing rate as a function of orientation under control conditions (black; OSI = 0.67; HWHH = 24 degrees) and during PV cell suppression (green; OSI = 0.59; HWHH = 26 degrees). Inset, left: the expansive nonlinear threshold or power law, i.e., the firing rate as a function of net membrane potential depolarization. Inset, right: orientation tuning curves in normalized to the peak. A 10% decrease in inhibition, as experimentally determined, results in ~50% increase in spiking response at the preferred orientation, a modest decrease in OSI (ΔOSI = 0.08), and a negligible change in tuning sharpness (ΔHWHH = 2 degrees).

PV cell activity with ChR2 demonstrates their further potential for linearly transforming visual responses in layer 2/3 of the cortex. Finally we showed, using in vivo whole-cell recordings, that the robust changes caused by PV cell perturbation on visually evoked responses in Pyr cells result from relatively small modulations in synaptic inhibition. A conductance-based model provides a likely explanation for how this small yet systematic change in inhibition can lead not only to the observed change in spiking response but also to the observed linear transformation.

Because of their powerful effect on firing rate, minor effect on direction and orientation selectivity and no systematic effects on tuning sharpness, PV-expressing interneurons appear ideally suited to modulate response gain in layer 2/3 of visual cortex (Figure 4). The results obtained here, therefore, provide a causal basis for the view that the response gain of neurons in visual cortex is under the control of GABAa mediated inhibition, as had been postulated based on pharmacological experiments (Katzner et al., 2011). Moreover, our experiments identify a specific role of PV cells in this control of response gain.

Quantification of PV Cell Perturbation

The changes in firing rate that we caused in PV cells are consistent with the changes in inhibitory conductance that we observed in Pyr cells. We chose to perturb PV cells over a moderate range, increasing or decreasing their activity by 3–4 spikes/s (i.e., ~40%; Figures 2D, 2E, and S2) of the average visual evoked firing rate of ~10 spikes/s (Figure 1D). Given that